



Calculations of Transverse Magnetic (TM) Wave Propagation between Strips in Different Shapes by using Finite Difference Time Domain (FDTD) Technique

Sedig S. Farhat

University of Tripoli, Faculty of Science, Department of Physics

Corresponding author: se.farhat@uot.edu.ly

ARTICLE INFO

Article history:

Received 22/01/2023

Received in revised form 14/05/2023

Accepted 27/05/2023

ABSTRACT

In this paper, the finite difference time domain (FDTD) technique was used in order to solve the time dependent Maxwell's curl equations in two-dimensional. The numerical simulations based on 2D-FDTD equations in transverse magnetic (TM_z) wave. We included many examples in this paper to demonstrate the propagation of (TM_z) wave between the strips in different shapes. Furthermore, the domain truncated by applied the second order approximate absorption condition to simulate unbounded problem to limit the region of a computational domain and minimize reflections that generated by four boundaries in 2D-FDTD. Therefore, the electric and magnetic field components of the TM_z waves propagated in 2D between the perfect electric conductors (PECs) and also distributions of the TM_z waves can be controlled when propagating the waves between the PECs. The results of simulations indicated that the waves propagated and concentrated between PECs in each branch design and the distributions can be changed. It means that the distributions of the fields can be produced in different patterns compared to the original excitation and also the wave propagation direction can be controlled between the strips. We obtained the same distributions when the waves propagated in the symmetrical structures. The results of simulations illustrated that the signals appeared identical when comparing the distributions of propagations in T-junction in the upper and lower parts. The results of the calculations showed that the phase can be changed between the strips..

Keywords: Maxwell's equations, Finite difference time domain (FDTD) technique, transverse magnetic (TM_z) wave, Second order Mur's absorbing boundary condition (ABC), Perfect Electric Conductor (PEC).

1. Introduction

There are many methods apply to solve the problems numerically in electromagnetic field. The finite difference time domain (FDTD) method is technique can be used to model a wide verity of electromagnetic problems in many applications, such as a mobile phone [1], propagation of electromagnetic wave in free space

and plasma [2]. The FDTD method published by Kane S. (1966), there are set of FDTD equations for the time dependent Maxwell's curl equations produced in two and three dimensions [3] and for example in 2D system set as the transverse electric (TE) and transverse magnetic (TM) modes. Therefore, the FDTD method will be applied to study several cases and also implemented the second order Mur's absorbing

boundary condition [4] which is very important in order to obtain very accurate results when terminating a computational domain. The aim of this paper is to study the propagation of TM_z wave between the strips made of perfect electric conductors (PECs) which can be constructed in two-dimensional system. For example, the distributions of TM_z waves can be studied by propagating the TM_z wave in a waveguide and T-junction in order to consider the distributions of the field components when propagating the wave from one channel to the next channel. The simulations were performed to demonstrate how the distributions of the field components will vary and also the distributions can be returned back to original excitation. This will be demonstrated and verified by the simulating using the FDTD method.

2. Method

The finite difference time domain (FDTD) method will be applied to solve Maxwell's equations in a two dimensions system and included a material such the PEC that behaviour as a copper. Therefore, the FDTD method can be employed to find a solution of Maxwell's equations numerically [3]:

$$\frac{\partial \mathbf{E}}{\partial t} = \frac{1}{\epsilon_0} \nabla \times \mathbf{H} \quad \dots\dots(1.a)$$

$$\frac{\partial \mathbf{H}}{\partial t} = -\frac{1}{\mu_0} \nabla \times \mathbf{E} \quad \dots\dots(1.b)$$

Where the ϵ_0 and μ_0 are the permittivity and permeability of a free space, respectively.

Equations (1) will be solved numerically because sometimes difficult to solve the problems analytically. We can study the propagation directions of TM waves by producing the waves inside a structure and varying the shape of the strips as this will lead to vary the distributions of the transverse magnetic waves. A comparison between the simulations can be observed by simulating different design. In this paper, the method will be used for example to study the propagations of electromagnetic waves between two parallel strips very close to each other and numerical calculation will show how to guide the wave in 2D system by solving Maxwell's equations and the system should be terminated by Mur's second-order absorbing condition (ABCs). Therefore, the ABCs use to truncate the computational domain in order to study an open region case. Therefore, the ABCs will be implemented in all calculation to reduce the reflections that generated by four edges. We wrote the MATLAB programs to solve

Maxwell's equations (2) numerically. In two dimensions (2D) system we can write Maxwell's equations as the transverse magnetic wave in free space as the following [3]:

$$\frac{\partial E_z}{\partial t} = \frac{1}{\epsilon_0} \left(\frac{\partial H_y}{\partial x} - \frac{\partial H_x}{\partial y} \right) \quad \dots\dots(2.a)$$

$$\frac{\partial H_x}{\partial t} = -\frac{1}{\mu_0} \frac{\partial E_z}{\partial y} \quad \dots\dots(2.b)$$

$$\frac{\partial H_y}{\partial t} = \frac{1}{\mu_0} \frac{\partial E_z}{\partial x} \quad \dots\dots(2.c)$$

Equation (2) will demonstrate the transverse magnetic wave (TM_z -polarized) and also Equation (2) should be normalized [5]. In the simulations will compute three electromagnetic field components in the x-y plane in each time step in each pixel. Equation (2) requires converting to discrete equations in order to implement in a computer program. Fig. 1 demonstrates the locations of the components based on the discrete Equation (3) which is called the two-dimensional updating equations. To obtain Equation (3), the central difference approximation method must be applied into Equation (2) for space and time. Therefore, the transverse magnetic (TM_z) mode can be given as set of equation on the x-y plane in discrete equations [3]:

$$H_x^{n+\frac{1}{2}}(i, j + \frac{1}{2}) = H_x^{n-\frac{1}{2}}(i, j + \frac{1}{2}) - \frac{\delta t}{\mu_0 \delta} (E_z^n(i, j + 1) - E_z^n(i, j)) \quad \dots\dots(3.a)$$

$$H_y^{n+\frac{1}{2}}(i + \frac{1}{2}, j) = H_y^{n-\frac{1}{2}}(i + \frac{1}{2}, j) + \frac{\delta t}{\mu_0 \delta} (E_z^n(i + 1, j) - E_z^n(i, j)) \quad \dots\dots(3.b)$$

$$E_z^{n+1}(i, j) = E_z^n(i, j) + \frac{\delta t}{\epsilon_0 \delta} \left(H_y^{n+\frac{1}{2}}(i + \frac{1}{2}, j) - H_y^{n+\frac{1}{2}}(i - \frac{1}{2}, j) \right) - \frac{\delta t}{\epsilon_0 \delta} \left(H_x^{n+\frac{1}{2}}(i, j + \frac{1}{2}) - H_x^{n+\frac{1}{2}}(i, j - \frac{1}{2}) \right). \quad \dots\dots(3.c)$$

Equation (3) will be utilized to generate the fields in the domain by using a point source acts as a hard source to excite a computational domain. In addition, to achieve very good results in the FDTD, the ABCs must be included in the computational domain as one of the significant concepts in the simulation when applying the FDTD Method because the advantage of ABCs is that the boundary condition can affect the final result and save time. Therefore, the boundary condition is very important to reduce any reflections when the signals reach at the end of the domain.

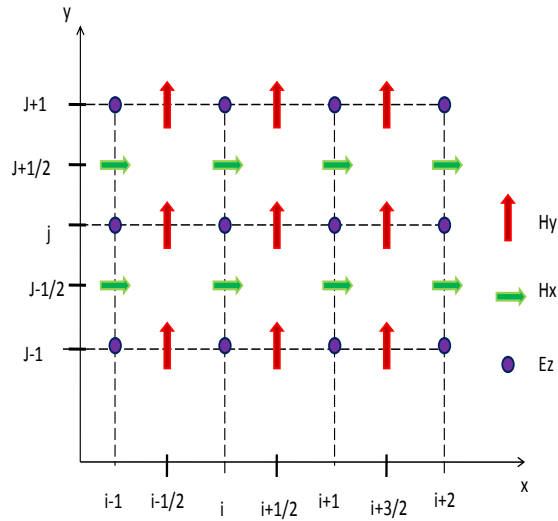


Figure 1: Positions of the electric and magnetic fields components in the two-dimensional FDTD mesh for the transverse magnetic (TM) mode [6]

In this calculations the computational domain will be terminated with the second Mur's absorbing boundary conditions (ABC) to simulate the structure surround an open region problem. It means that the wave should be propagated in a space without reflections back to a domain. The second orders Mur's boundary condition in the two-dimensional will set as the discrete equations at the boundary $x=0$, $x=x_{max}$, $y=0$ and $y=y_{max}$ by applying the following forms in a uniform mesh ($\Delta x = \Delta y = \delta$) in a grid in 2D system [4]:

$$E_z^{n+1}(0, j) = -E_z^{n-1}(1, j) + \frac{(c \delta t - \delta)}{(c \delta t + \delta)} (E_z^{n+1}(1, j) + E_z^{n-1}(0, j)) + \frac{2\delta}{c \delta t + \delta} (E_z^n(0, j) + E_z^n(1, j)) + \frac{(c \delta t)^2}{2\delta(c \delta t + \delta)} (E_z^n(0, j + 1) + E_z^n(0, j - 1) - 2E_z^n(0, j) + E_z^n(1, j + 1) + E_z^n(1, j - 1) - 2E_z^n(1, j)) \quad \dots\dots\dots(4.a)$$

$$E_z^{n+1}(h, j) = -E_z^{n-1}(h - 1, j) + \frac{(c \delta t - \delta)}{(c \delta t + \delta)} (E_z^{n+1}(h - 1, j) + E_z^{n-1}(h, j)) + \frac{2\delta}{c \delta t + \delta} (E_z^n(h, j) + E_z^n(h - 1, j)) + \frac{(c \delta t)^2}{2\delta(c \delta t + \delta)} (E_z^n(h, j + 1) + E_z^n(h, j - 1) - 2E_z^n(h, j) + E_z^n(h - 1, j + 1) + E_z^n(h - 1, j - 1) - 2E_z^n(h - 1, j)) \quad \dots\dots\dots(4.b)$$

At $y=0$

$$E_z^{n+1}(i, 0) = -E_z^{n-1}(i, 1) + \frac{(c \delta t - \delta)}{(c \delta t + \delta)} (E_z^{n+1}(i, 1) + E_z^{n-1}(i, 0)) + \frac{2\delta}{c \delta t + \delta} (E_z^n(i, 0) + E_z^n(i, 1)) + \frac{(c \delta t)^2}{2\delta(c \delta t + \delta)} (E_z^n(i + 1, 0) + E_z^n(i - 1, 0) - 2E_z^n(i, 0) + E_z^n(i + 1, 1) + E_z^n(i - 1, 1) - 2E_z^n(i, 1)) \quad \dots\dots\dots(4.c)$$

At $y=y_{max}$

$$E_z^{n+1}(i, h) = -E_z^{n-1}(i, h - 1) + \frac{(c \delta t - \delta)}{(c \delta t + \delta)} (E_z^{n+1}(i, h - 1) + E_z^{n-1}(i, h)) + \frac{2\delta}{c \delta t + \delta} (E_z^n(i, h) + E_z^n(i, h - 1)) + \frac{(c \delta t)^2}{2\delta(c \delta t + \delta)} (E_z^n(i + 1, h) + E_z^n(i - 1, h) - 2E_z^n(i, h) + E_z^n(i + 1, h - 1) + E_z^n(i - 1, h - 1) - 2E_z^n(i, h - 1) + E_z^n(i - 1, h - 1)) \quad \dots\dots\dots(4.d)$$

There are many types of boundaries conditions such as truncation condition and Mur's boundary condition. The latter is a radiation boundary condition which will minimize any reflection at the four edges when updating a system in each time step by Equation (4). It means that four sides can be truncated the problem space at the $x=0$, $x=x_{max}$, $y=0$ and $y=y_{max}$ boundaries. Moreover the equation (3) will be utilized to generate the TM_z waves that controlled to propagate between two strips made of perfect electric conductors (PECs). It will be noted that during the calculation the PECs boundaries will performance as a metal material strip such as the copper. This can be done by setting the electric field component at the locations of PECs equal zeros during the calculations in all time steps. Therefore, we expect that the waves will focus to propagate between the PECs as constructed in different design in a space. By using this approach many shapes can be constructed as a mesh mode to consider the propagation of electromagnetic waves such as simulating a one line consists of two parallel strips and then connecting to T-junction and also T-junction will be connected to two elements and each element consists of two parallel strips. We expect that the last model will lead to vary the patterns of the TM_z components when propagating from one branch to next branch. Therefore, the numerical simulations results will be provided for a number of examples as will be seen in the result section.

3. Results and Discussion

In this section, we will demonstrate the results generated in the x - y plane based on sets of Equations (3). In the following calculation, the 2-D FDTD programs wrote by using MATLAB (R2013a) programming languages to simulate the TM_z waves propagate in a free space and also the computational domain can be truncated by the radiation boundary condition that provided by Equation (4). In each program can be written to simulate the fields as the following, we set a problem space, define the parameters, calculate the fields coefficients, update the electric field component, update the magnetic field components and update the absorbing boundary conditions (ABCs) in every time step during the calculations and finally data analysis. There are many similar studies that have applied the ABCs to truncate the computational domain in order to reduce any reflections produce by the boundaries. It can be truncated a domain as the examples by using a perfectly matched layer (PML) [7], first order Mur's boundary condition [8] and second order Mur's boundary condition [9].

We will set the computational space to be 200×200 cells in the x and y directions. The cell size should be equal to twenty sample points per wavelength in order to achieve very good results and the Courant stability condition should be applied [10, 11]. Fig. (2) demonstrates a first example, a hard source with the sinusoidal signal operated at 10 GHz was chosen for excitation a domain and source was placed in the centre of a space. In this calculation there is no absorbing boundary condition ABCs were included in the lower side, upper side, left side and right side of the domain as shown in fig. 2 (A, B, C D), respectively. When there are no the ABCs included in the all sides in the calculations as shown in fig. 2 (E), it can be observed that the distributions have changed in the calculation. Therefore, one should notice that the distribution will be appeared different as shown in fig. 2 (E) and the uniformity of the TM field components disappeared at the walls when compared fig. 2 (E) with fig. 2 (F). This is due to the fact that the waves are transmitting from the source and then the wave reflected back to the domain when reached the four walls. We can improve the simulation results and overcome this difficulty by including an absorbing boundary condition in the calculations. As a result, very important to truncate a space by the second-order's Mur ABCs as shown in fig. 2 (F). The calculations generated in the same time steps (275) for a comparison of the simulations. It can be said that the calculations demonstrated that the absorbing boundary condition is very significant to acquire good time domain data. Therefore, figure 2 (F) shows very good simulation result that obtained once the ABC included in the calculations by implemented Equation (4) in the calculation. One can easily observe that we are able to obtain circular radiations patterns as clearly demonstrated in fig. 2 (F) that compared to fig. 2 (A, B, C, D and E) as there were appeared deformations at proximity to the boundaries.

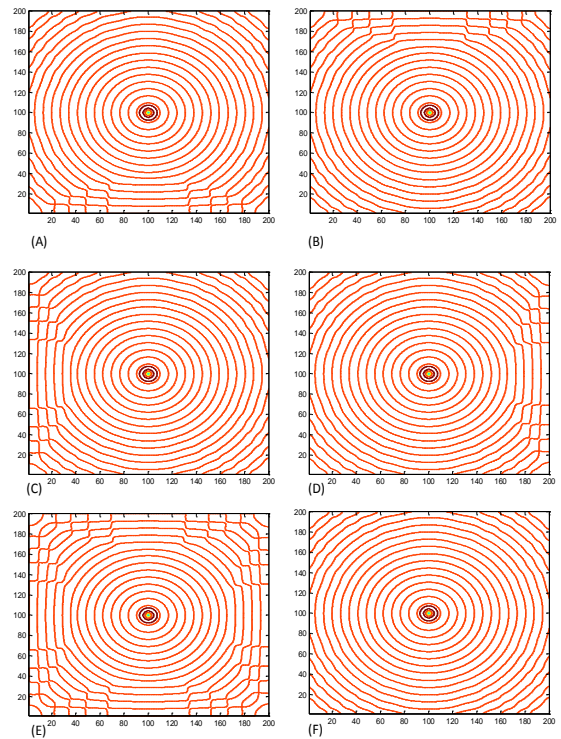


Figure 2: Contours plots of the electric field component, the images clearly illustrate that there are no absorbing boundaries as demonstrated: (A), (B), (C), (D)) on the lower side, upper side, left side, right side and (E) without ABCs on all sides and (F) ABCs included on the four sides

Moreover, there are several shapes can be constructed in 2-D system such as a waveguide of the TM wave by two parallel strips as shown in fig. 3 (A), the waveguide connected with T-junction as shown in fig. 3 (B) and two strips have the same dimensions connected in the lower and upper regions of the T-junction as shown in fig. 3 (C). It can control the signal to propagate in the left side or right side of the structure based on the location of the source as shown in fig. 3 (D). Because, the source will generate the signal bilaterally, it means that the wave generates in the positive and negative directions. Moreover, it can be controlled the signals to propagate in the upper region or lower region by inserting a gate have a property of a PEC between the strips and the gate can be placed in the middle of the structure as shown in figure 3 (E and F). Moreover, it can be generated the signal out of phase when the upper and lower structure in T-junction is not identical and also we can control the intensity of the field by changing the size of gate. Therefore, we described how to construct many designs that are demonstrated as a mesh mode as shown in fig. 3. We will expect that the TM waves will focus to propagate through a shape between the PECs strips. The propagation of the waves will take many different paths depend on the shape design. Therefore, many examples will display the directions of

propagations of the signals within each structure. It can be seen that the arrows in fig. 3 referred to the directions of propagation in each design. Many shapes will be simulated as example, waveguide, T-junction, U-shape and waveguide as shown in fig. 3 (A, B, C, D, E and F, respectively).

The first example, the field components were generated and can be observed that there is a higher field value of the H_y at the edges of a waveguide while the other field components concentrated in the centre of the waveguide as shown in fig. 4. The second study is that T-junction design as shown in fig. 5 and T-junction connected to the waveguide. Therefore, the signal propagated between the strips until reached to T-junction and propagated into the upper and lower parts of T-junction as shown in fig. 5. This type of shape will change the distributions compared with the signals propagate in the first simulation. The third simulation, we can control signals to propagate in upper region or lower region by adding a gate to control the direction of propagation on 90° degree. for a example when the closed lower region by placed a gate as shown in fig. 6, the signal propagated in the upper region while propagating in lower region when the closed the gate in the upper region as shown in fig. 7. It means that the directions of wave propagations rotated 90 degrees.

We designed the U-shape as shown in fig. 8, the signal propagated until reached the end of the T-junction after that the waves propagated inside two branches in the upper and lower regions between two strips have the same length and width as shown in fig. 8. It can be noted that, the patterns have returned back as a first pattern of propagation in the first simulation. The pervious simulation considered as the first case as we designed the length of T-junction in the lower and upper parts have the same lengths from the centre of the main branch. The second case is that the length of upper region less that the lower region in the T-junction as shown in fig. 9. It can be noted that there is the difference appeared in the distributions of TM wave as observed that the waves appeared out of phase when comparing the simulations results that calculated in fig. 8. The next simulation can explain that the amount of signals can be controlled as propagated in each element by varying the size of the gate as shown in fig. 10.

Therefore, the intensity of the TM field components in the bottom branch is a little in comparison to the upper branch. By increasing the width between the strips, the distributions of TM waves have changed as shown in fig. 11 when comparing the upper with lower regions. Results of the simulations can indicated that the signals can be propagated in two branches with different

distributions and the signals intensity appeared slightly different. Moreover, the TM waves can be propagated and rotated between the strips as the signals will control to propagate in the upper branch or lower branch based on the location of a gate as illustrated in fig. 12 and fig. 13, respectively. Furthermore, the waves have propagated from the left region to the right region as described in the previous simulations. Finally, it can be designed the structure to allow the wave to propagates from right region to left region for a example from the upper branch and then propagating in T-junction after that the wave propagated to the left region during the main branch and also the signal propagated to the right through the bottom branch then spreading out in free space as shown in fig. 14.

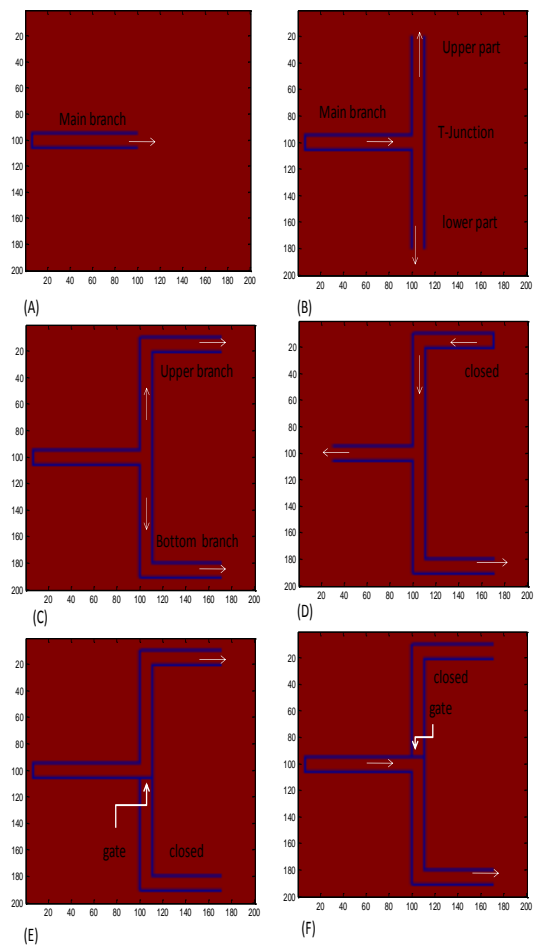


Figure 3: The use of PECs to construct a number of shapes as a mesh mode. Note: the arrows indicate the wave propagation directions

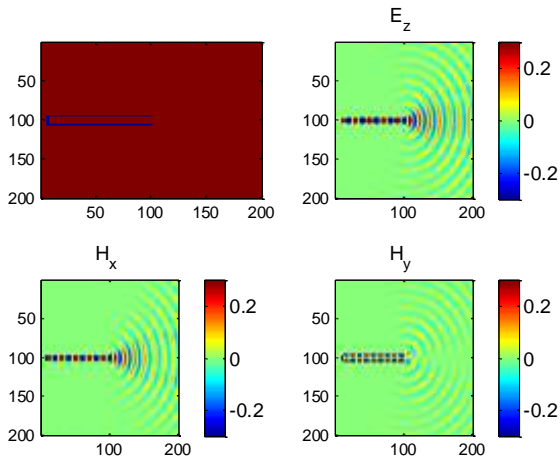


Figure 4: The TM_z components generated between the two strips at 575 time steps and the second-order Mur's absorbing boundary condition applied to all sides

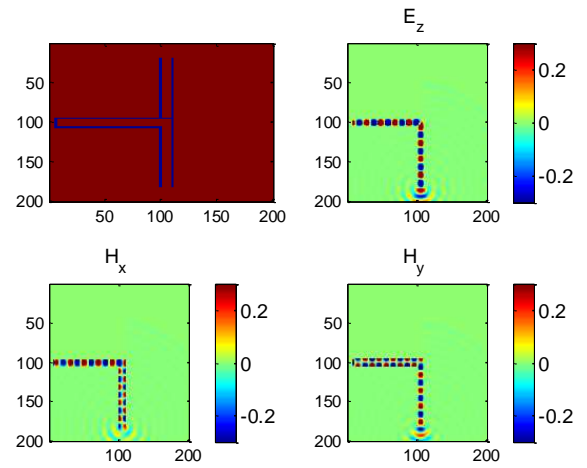


Figure 7: The waveguide: the gate is located parallel to the upper strip and the signals propagated in the lower part in the T-junction at 575 time steps

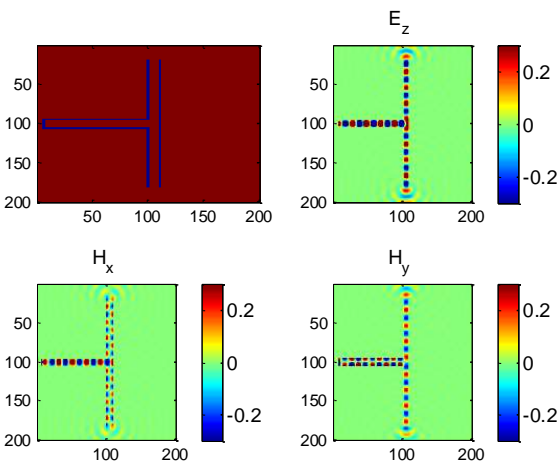


Figure 5: The TM_z components are generated between two strips at 575 time steps and then propagating through T-junction and the original pattern generated in main branch has changed in the T-junction

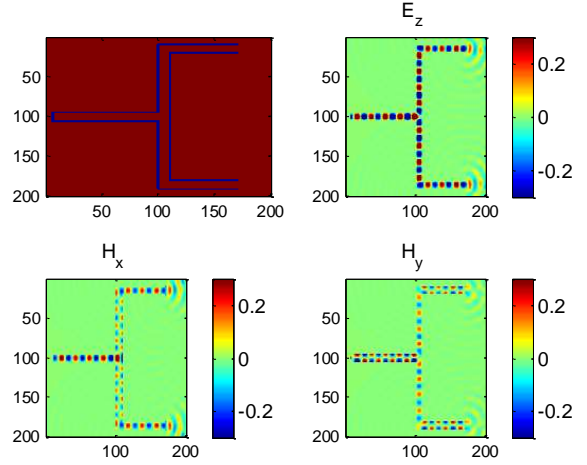


Figure 8: U-shape: Signals generated at 788 time steps between the two strips on the left and propagated into T-junction and then propagated on the top and bottom branches into two elements. The signal returned to original pattern on the top and bottom branches

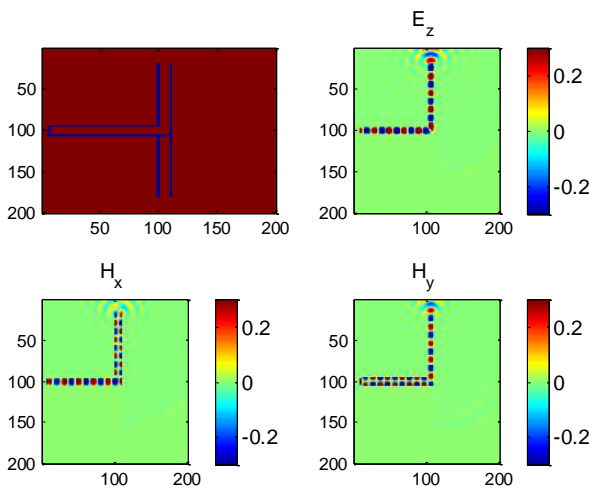


Figure 6: The waveguide: the gate is located parallel to the lower strip and the signals propagated at directly to the upper part in the T-junction at 575 time steps

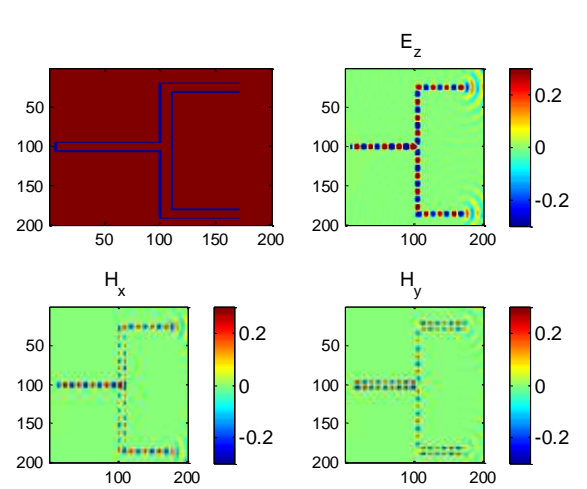


Figure 9: U-shape: signals generated at 788 time steps between two strips and then connected with T-junction have different length and then propagating on the top and bottom branches and the signals appeared out of phase compared to previous simulation

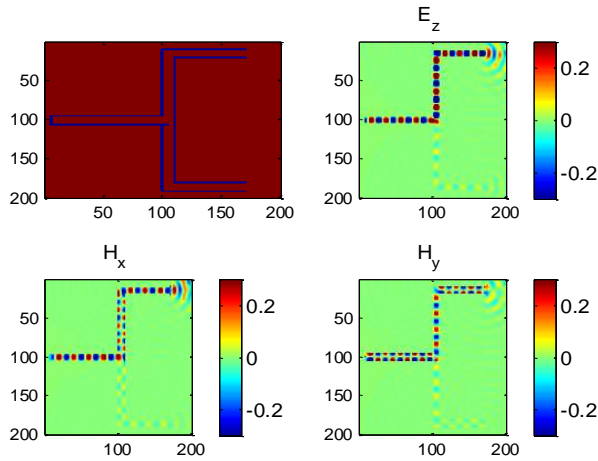


Figure 10: The gate is located parallel to the lower strip and the size of the gate is controlled and signals propagated in the lower and upper regions with the different intensity at 788 time steps

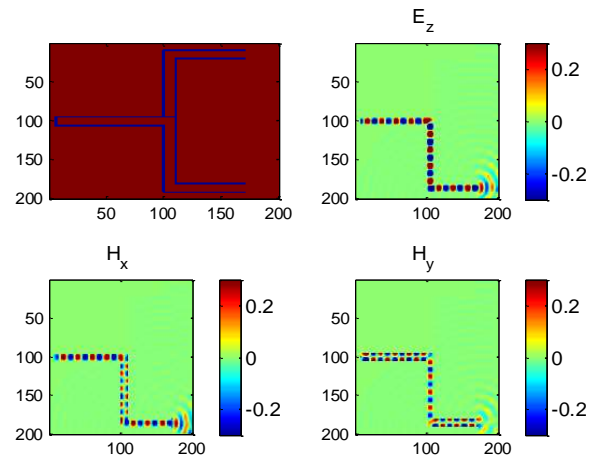


Figure 13: The gate is located parallel to the upper strip and signals propagated in the bottom region on the lower branch

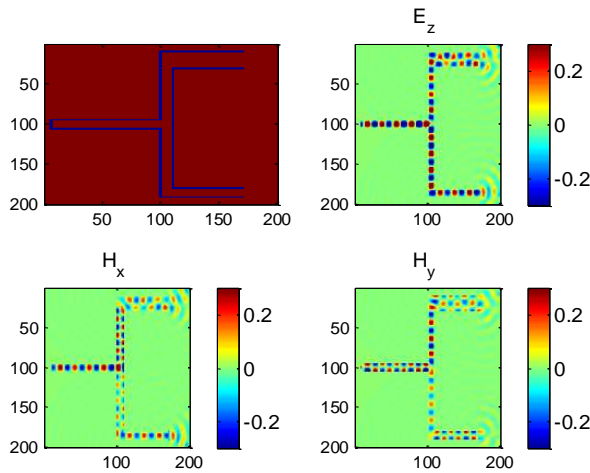


Figure 11: Signals generated at 788 time steps between two strips and signals propagated in T-junction and then propagated on the top and bottom branches have different width and the mode of the signals appeared difference compared to previous simulations

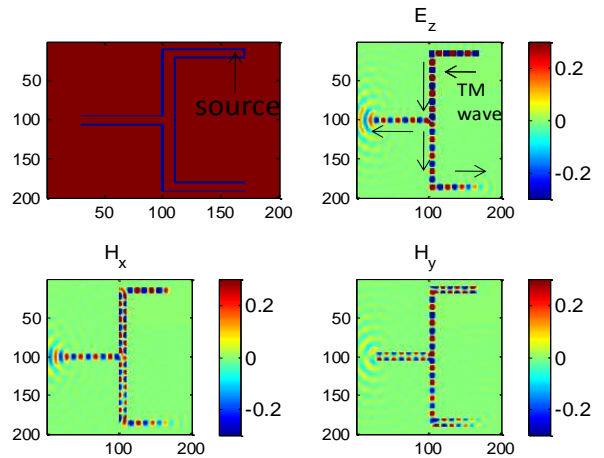


Figure 14: The top branch is closed and signals propagated on the left side until reached to T-junction to propagate in this region until reach in the middle branch propagated on the left and also propagating to the bottom branch

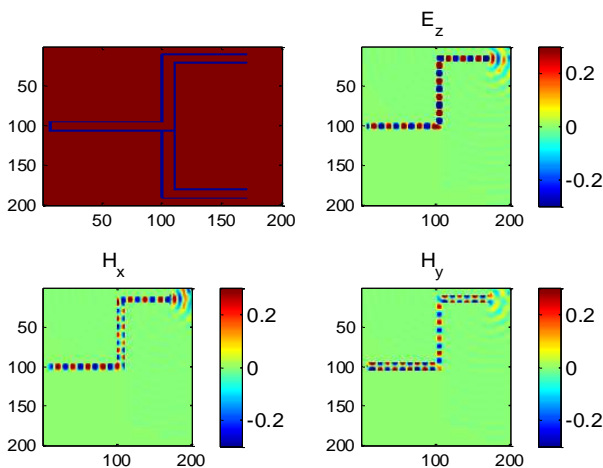


Figure 12: The gate is located parallel to the lower strip and the signals propagated in the upper region

4. Conclusion

In this paper, we described the implementation of the two-dimensional 2D-FDTD equations with including the second order Mur's absorbing boundary condition (ABC) in calculations. It can be concluded that the finite difference time domain method is very good technique to explain how the waves propagated in the two-dimensional system between the strips. Therefore, the FDTD method is appropriate for solving Maxwell's equations. The numerical calculations showed that the FDTD is very powerful technique to model the two-dimensional structure in different shapes. This paper presented the effect of ABCs as the system terminated by using the second-order's Mur ABC and the results of simulations indicated that good numerical performance of the ABC. Therefore, it was found that this boundary

is very good approximation approach to employ for simulating the 2-D FDTD as well as the ABCs must be applied in the calculations in order to save the computational time.

5. References

- [1] Khitam, Y. E., Sami, A. A. and Mohammed, M. S. (2018). 3D-FDTD Head Model Exposure to Electromagnetic Cellar Phones Radiation. American Journal of Electromagnetic and Application, 6, 42-48.
- [2] Jeahoon C., Min S. P. and Jung K. (2022). Numerical accuracy of finite difference time domain formulations for magnetized plasma. Journal of electromagnetic engineering and science, 22, 3, 195-201.
- [3] Yee, K. S. (1966). Numerical Solution of Initial Boundary Value Problems Involving Maxwell's Equations in Isotropic Media. IEEE Transaction on Antenna Propagation, 14, 302-307.
- [4] Mur G. (1981). Absorbing Boundary Conditions for the Finite Difference Approximation of the Time Domain Electromagnetic field equations. IEEE Transactions on Electromagnetic Compatibility, EMC-23, 377-382.
- [5] Arnold A., Y. Yue and Wang M. (2020). Non-Split Perfectly Matched Layer Boundary Condition for Numerical Solution of 2D Maxwell Equations, International Journal of Electromagnetic (IJLE), 3, 1, 1-9.
- [6] Hendi A., Alkallas F., Almoussa H., Alshahri H. and Almoneef M. (2020). Finite difference time domain method for simulating dielectric materials and metamaterials. Digest journal of nonomaterialand biostructures, 15, 3, 707-719.
- [7] Berenger J. P. (1994). A perfectly matched layer for the absorption of electromagnetic waves. Journal of computational physics, 114, 185-200.
- [8] William J. and Gupta N. K. (1994). Application of 3D finite difference time domain (FDTD) method to predict radiation from a PCB with high speed pulse propagation. Conference paper IEEE, 287-291.
- [9] Korada U. and Taflove A. (1982). Novel method to analyze electromagnetic scattering of complex objects. IEEE, 24, 4, 397-405.
- [10] Taflove A. and Morris E. (1975). Numerical Solution of Steady State Electromagnetic Scattering Problems using the Time Dependent Maxwell's Equations. IEEE Transaction on Microwave Theory and Techniques, 23, 623-630.
- [11] Otman S. and Ouaskit. S. (2017). FDTD Simulations of Surface Plasmon using the effective Permittivity applied to the dispersive Media. American Journal of Electromagnetic and Applications, 5, 14-19.